energies

MDPI

Article

Determining the Seasonal Variability of the Territorial Sea Baseline in Poland (2018–2020) Using Integrated USV/GNSS/SBES Measurements

Mariusz Specht [1], Cezary Specht [2], Andrzej Stateczny [3,*], Łukasz Marchel [4], Oktawia Lewicka [2], Monika Paliszewska-Mojsiuk [5] and Marta Wiśniewska [6]

1 Department of Transport and Logistics, Gdynia Maritime University, Morska 81-87, 81-225 Gdynia, Poland; m.specht@wn.umg.edu.pl
2 Department of Geodesy and Oceanography, Gdynia Maritime University, Morska 81-87, 81-225 Gdynia, Poland; c.specht@wn.umg.edu.pl (C.S.); o.lewicka@wn.umg.edu.pl (O.L.)
3 Department of Geodesy, Gdańsk University of Technology, Gabriela Narutowicza 11-12, 80-233 Gdańsk, Poland
4 Department of Navigation and Hydrography, Polish Naval Academy, Śmidowicza 69, 81-127 Gdynia, Poland; l.marchel@amw.gdynia.pl
5 Confucius Institute, University of Gdańsk, Jana Bażyńskiego 8, 80-309 Gdańsk, Poland; monika.paliszewska@ug.edu.pl
6 Marine Technology Ltd., Wiktora Roszczynialskiego 4-6, 81-521 Gdynia, Poland; m.wisniewska@marinetechnology.pl
* Correspondence: andrzej.stateczny@pg.edu.pl

Citation: Specht, M.; Specht, C.; Stateczny, A.; Marchel, Ł.; Lewicka, O.; Paliszewska-Mojsiuk, M.; Wiśniewska, M. Determining the Seasonal Variability of the Territorial Sea Baseline in Poland (2018–2020) Using Integrated USV/GNSS/SBES Measurements. *Energies* **2021**, *14*, 2693. https://doi.org/10.3390/en14092693

Academic Editor: Jae-Young Pyun

Received: 17 March 2021
Accepted: 4 May 2021
Published: 7 May 2021

Abstract: The Territorial Sea Baseline (TSB) allows coastal states to define the maritime boundaries, such as: contiguous zone, continental shelf, exclusive economic zone and territorial sea. Their delimitations determine what rights (jurisdiction and sovereignty) a given coastal state is entitled to. For many years, the problem of delimiting baseline was considered in two aspects: legal (lack of clear-cut regulations and different interpretations) and measurement (lack of research tools for precise and reliable depth measurement in ultra-shallow waters). This paper aimed to define the seasonal variability of the TSB in 2018–2020. The survey was conducted in three representative waterbodies of the Republic of Poland: open sea, river mouth and exit from a large port, differing between each other in seabed shape. Baseline measurements were carried out with Unmanned Surface Vehicles (USV), equipped with Global Navigation Satellite System (GNSS) geodetic receivers and miniature Single Beam Echo Sounders (SBES). The survey has shown that the smallest seasonal variability of TSB (1.86–3.00 m) was confirmed for the waterbody located near the Vistula Śmiała River mouth, which features steep shores. On the other hand, the greatest variability in the baseline (5.73–8.37 m) as observed in the waterbody adjacent to the public beach in Gdynia. Factors conditioning considerable changes in TSB determination were: periodically performed land reclamation works in the area and the fact that the depth of the waterbody increases slowly when moving away from the coastline.

Keywords: Territorial Sea Baseline (TSB); Unmanned Surface Vehicle (USV); Global Navigation Satellite System (GNSS); Single Beam Echo Sounders (SBES); hydrographic surveys; coastal waters

1. Introduction

According to international law, boundary delimitation means establishing boundaries between states. For sea areas, a coastal state may draw four types of maritime boundaries: contiguous zone, continental shelf, exclusive economic zone and territorial sea [1,2]. Due to the possible occurrence of natural resources at sea areas, determining jurisdiction of coastal states is currently one of the most important issues in international relations. The prerequisite is to draw a Territorial Sea Baseline (TSB), without which it is impossible to determine maritime boundaries of sea areas connected with it [3,4] (Figure 1).

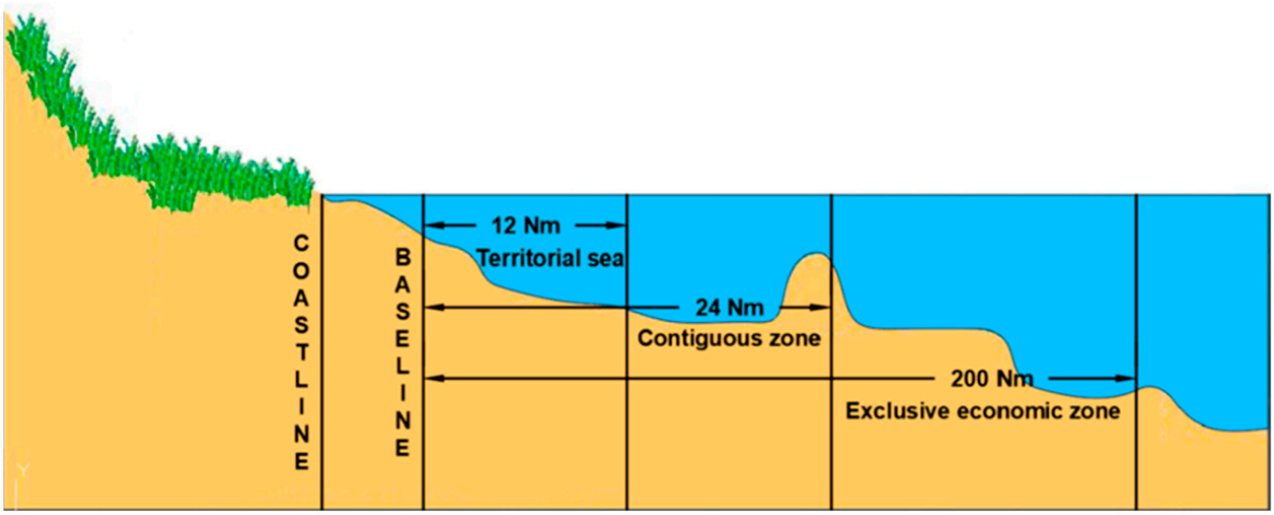

Figure 1. Limits of maritime zones. Own study based on [5].

The baseline can be defined in two ways in the literature. The first is that when the coastline is regular then the TSB is defined as: "*the low-water line along the coast as marked on large-scale charts officially recognized by the coastal state*" [6]. In the latter case, the baseline is straight, and it can be used: "*In localities where the coastline is deeply indented and cut into, or if there is a fringe of islands along the coast in its immediate vicinity*" and "*Where because of the presence of a delta and other natural conditions the coastline is highly unstable*" [6]. Thus, this line is used only when the coastline is varied.

To date, coastal states have considered drawing baselines in two aspects only: legal and measurement. For example, in Poland, pursuant to the Regulation of 2017 [7], the current Polish maritime boundary is determined based on the legal acts of 1957–1995. In such a case, it should be recognized that data defining the drawing of a TSB is out of date, which is conditioned, first and foremost, by the variability of hydrological conditions of the Baltic Sea. The second issue pertains to the methodology of performing baseline measurements. In connection with the fact that the TSB is located in ultra-shallow waters, featuring depths of below 1 m, classical geodetic methods were used to determine its course. Among them, the following may be distinguished: tachymetric methods (popular until 1990) [8], Differential Global Positioning System (DGPS) (positioning accuracy of 1–2 m, $p = 0.95$), Real Time Kinematic (RTK) systems using the Global Positioning System (GPS), and direct measurements taken by land surveyors with profiles performed in the sea water [9,10]. The measurement methods listed above were of low efficiency due to accuracy of the conducted survey, small area coverage with measurements and the survey duration.

Only recently has the development of measurement techniques taken place, allowing for the execution of TSB measurements. Among them, the following may be distinguished: Unmanned Surface Vehicles (USV), which are characterized by high maneuverability and small sizes [11–18], Global Navigation Satellite System (GNSS) geodetic networks providing services of both real-time, as well as post-processing [19–23] and miniature devices for depth measurements [24–28]. Thanks to them, it is possible to carry out bathymetric measurements in ultra-shallow waters with up to centimeter accuracy [29–31], as well as in a rapid and reliable manner. Moreover, photogrammetric methods are often used to analyze coastal zone changes, using unmanned [32–36] and manned aircrafts [37], as well as analyzing multispectral images of high [38–41] and moderate [42,43] resolution.

The paper features the following structure. Chapter 2 is a description of three representative waterbodies of the Republic of Poland, on which TSB measurements are taken. Additionally, this section presents measurement equipment, used for surveying the seasonal variability of the baseline. Moreover, this chapter describes the method of performing TSB measurements and defines the method of elaborating measurement data, registered during the survey. In chapter 3, baseline course is visualized for the three waterbodies of

the Republic of Poland and a discussion is held over the issue of how Poland's TSB has changed over the course of years. The article is summed up with final (general) conclusions, summarizing the paper's content.

2. Materials and Methods

2.1. Measurement Locations

TSB measurements are performed in coastal sea areas, characterized by small depths [6,7]. In the case of Poland, the baseline is located at a depth of several dozen cm to 1–2 m below the current water level. Its position depends on the water level fluctuations and seafloor shape of the waterbody. In connection with the above, it was decided to select three representative waterbodies of the Republic of Poland for TSB measurements to be taken (Table 1).

Table 1. Representative waterbodies on which TBS measurements were carried out [44].

Name of Waterbody	Features	Photograph
Waterbody No. 1: Open sea public beach in Gdynia	A waterbody with a typically running, straight coastline. The waterbody length is about 450 m.	
Waterbody No. 2: Vistula Śmiała River mouth near the National Sailing Centre (NSC) in Gdańsk	A waterbody of great dynamics of hydromorphological features (with no hydrotechnical structures). The waterbody length is about 250 m.	
Waterbody No. 3: Exit from a large port area near the entrance to Górki Zachodnie from the Gdańsk Bay	A waterbody with a large number of hydrotechnical structures. The waterbody length is about 250 m.	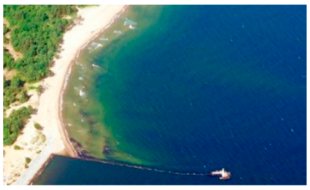

Depending on the location of baseline measurement, a sounding profile arrangement had to be designed. They were indicated pursuant to the recommendations set forth in the standard issued by the International Hydrographic Organization (IHO), entitled "IHO Standards for Hydrographic Surveys" [45]. It was decided to design main profiles perpendicular to the direction of coastline, with an assumption that distances between the profiles will amount to 5–10 m. Moreover, to verify the conducted survey, control profiles were determined every 10–20 m, which were perpendicular to main profiles [44]. Figure 2 presents the sounding profile arrangement for three waterbodies of the Republic of Poland.

For scheduling hydrographic surveys, Trimble Business Center (TBC) software and ortophotos shared on Google Earth Pro platform were used. It must be taken into account that the sounding profile arrangement during individual measurement campaigns might have changed slightly due to shifts in coastline, both for inland, as well as towards the sea. This situation was particularly evidenced in waterbody No. 2, where the greatest changes in coastline were observed.

(**a**)

(**b**)

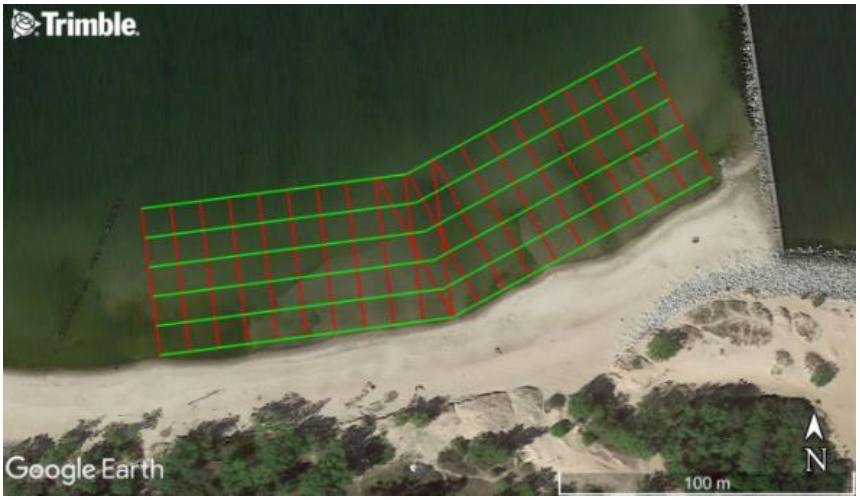

(**c**)

Figure 2. The sounding profile arrangement for representative waterbodies: (**a**) No. 1; (**b**) No. 2; (**c**) No. 3 [44].

2.2. Measurement Equipment

For the execution of TSB measurements, a research tool (developed at the beginning of the 2010s) was used, i.e., a hydrographic USV. This is a radio remote control vessel, providing for hardware integration with a GNSS phase receiver and vertical echosounder (minimum equipment). It is designed for conducting hydrographic surveys of docks, lakes, rivers and small water reservoirs. For the survey, two unmanned surface vehicles were used: an OceanAlpha USV SL20 (OceanAlpha Group Ltd., Hong Kong, China) in an autonomous version and a Seafloor Systems HyDrone (Seafloor Systems Inc., Shingle Springs, CA, USA) in an autonomous version (after modernization of the remote-control mode) (Figure 3). They feature many benefits, in comparison to manned vessels, including high maneuverability and small sizes, making it possible to navigate over tight routes. Additionally, a major benefit of unmanned vessel is a pump-jet drive, which renders it possible for them to navigate in waterbodies overgrown with aquatic vegetation, e.g., reeds.

(**a**) (**b**)

Figure 3. USVs: (**a**) OceanAlpha USV SL20; (**b**) Seafloor Systems HyDrone.

For registration of measurement data, miniature Single Beam Echo Sounders (SBES) were used [SBES series Echologger (Teledyne RD Instruments Inc., Poway, CA, USA) and SonarMite BTX (Ohmex Ltd., Lymington, UK)], allowing to measure depths of up to 30 cm with an accuracy of centimeters and GNSS geodetic receivers [Leica Viva GS 15 (Leica Geosystems, St. Gallen, Switzerland) and Trimble R10 (Trimble Inc., Sunnyvale, CA, USA)], making it possible to determine position coordinates with an accuracy of a couple of centimeters. To navigate unmanned surface vehicles in autonomous mode, autopilots (PixHawk Cube) were used, supported by GNSS receivers and magnetic compasses. Based on the previously conducted surveys, it was established that both control systems provide for the possibility of maintaining USV on sounding profiles with an accuracy of: 0.92–2.11 m (p = 0.68) and 2.01–2.72 m (p = 0.95) [46,47].

2.3. TSB Measurements

Since an important factor influencing the obtained results are hydrometeorological conditions, the measurements were taken in windless weather conditions and with calm water (0 in the Douglas sea scale, no wave nor sea currents). When a favorable weather window was forecast, the survey was conducted. Before starting any measurement campaign, the measurement equipment had to be mounted (miniature SBES and GNSS geodetic receiver) on the USV. After the mounting of sensors on the unmanned surface vehicle, they must be calibrated in order to function properly. Hence, for the miniature SBES, the following three operations were carried out [48]:

1. Calibration (taring) of the vertical echo sounder;
2. Measurement of the vertical distribution of the speed of sound in water;

3. Measurement of the draft of the echo sounder transducer.

However, for the GNSS geodetic receiver, the following two operations were performed:

1. Inclinometer calibration;
2. Magnetometer calibration.

When all the above-listed tasks had been completed, a significant number of measurements were then taken. For the survey, five measurement campaigns were carried out, with each waterbody being measured three times. Detailed information about the conducted measurements is provided in Table 2.

Table 2. Information on the conducted measurement campaigns of the TSB.

Measurement Campaign Number	Measurement Date	Measurement Location	Number of Recorded Points	Measurement Equipment
1	19 July 2018	Waterbody No. 1	7204	 USV: Seafloor Systems HyDrone (after modernization) Autopilot: PixHawk Cube Echosounder: SonarMite BTX GNSS receiver: Trimble R10
2	18 September 2018	Waterbody No. 2	4655	
		Waterbody No. 3	3446	
3	25 July 2019	Waterbody No. 2	4048	
		Waterbody No. 3	3029	
4	19 September 2019	Waterbody No. 1	8163	
5	8 October 2020	Waterbody No. 1	7204	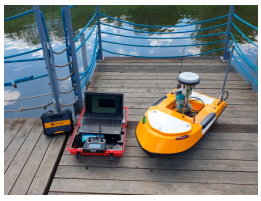 USV: OceanAlpha USV SL20 Autopilot: Not specified Echosounder: Echologger series SBES GNSS receiver: Leica Viva GS 15
		Waterbody No. 2	3680	
		Waterbody No. 3	3741	

2.4. Measurement Data Elaboration

After having taken the measurements, it was decided to transform the registered data into a single, three-dimensional coordinate system. Among others, Gauss–Krüger projection, Universal Transverse Mercator (UTM) coordinate system, Kronstadt 86 height system and PL-geoid2011 quasigeoid model was used for the survey. All transformations of coordinates of points were conducted with TBC software.

The depths were then registered with an echosounder for the chart's datum (508 cm) were to be checked. To this end, the values of water levels, as shared by the Polish Institute of Meteorology and Water Management-National Research Institute (IMWM-NRI), were used. To indicate the current water level, information from the gauging station, located the closest to the site of hydrographic surveys, was utilized. Thus, in the case of waterbody No. 1, it was the tide gauge located in Gdynia; and for waterbodies No. 2 and 3, it was the gauging station in Gdańsk-Port Północny [44].

Following measurement data preparation, elaboration of numerical seabed models in the surveyed waterbodies started. For their preparation, TBC was used, making it possible to generate the surface of an area in the form of Triangulated Irregular Network (TIN). A TIN model is generated through the triangulation of depth points, fulfilling the Delaunay condition that a circle circumscribed around a triangle contains only the vertices of the triangle. In other words: inside such a circle there are no other points that do not belong to the triangle about which the circle was circumscribed. This characteristic makes the

Delaunay triangulation exceptional, and it is implemented in various applications. For the purpose of this paper, it will be used for three-dimensional modelling of the seabed in the coastal zone [49–52]. The outcome of the triangulated irregular network model will be tetrahedrons connected with each other. An exemplary model in the form of TIN is presented in Figure 4. Other popular seabed modelling methods in hydrography are GRID, B-splines and NURBS [53–55].

A TIN model was used in the calculations for several reasons. Firstly, the authors did not care about excessive smoothing of the waterbody in the unmeasured areas. Secondly, the proximity of the measured waterbodies and the land resulted in large variability in bathymetry. In this case, the use of methods characterized by a tendency to smooth data would have the result that these areas could be mapped in a manner deviating from reality. Another reason for the use of TIN is that the USV had a tendency to constantly change the speed. In this case, methods such as kriging would give more weight to observations made at lower velocities (density of measurements), and areas measured at higher speeds would have lower weights. Such a phenomenon would cause excessive smoothing of areas measured at high velocities.

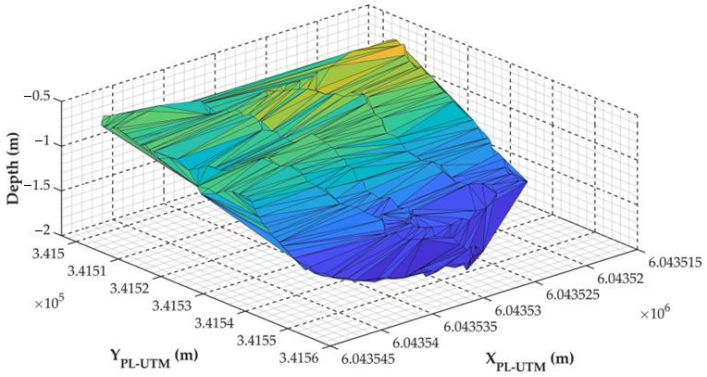

Figure 4. Seabed of the waterbody No. 1 in the form of a TIN.

The next step was to define the TSB depth in the surveyed waterbodies. To accomplish this, pursuant to the definition in Article 5 of the United Nations Convention on the Law of the Sea (UNCLOS), the lowest water level ever registered along the coast of a given coastal state should have been identified [6]. Therefore, for the purpose of this paper, information on the lowest water levels ever registered at Polish gauging stations in 1945–2015 were obtained from the Maritime Department of the IMWM-NRI in Gdynia. In the case of waterbody No. 1, the lowest water level was 415 cm (registered on 04 November 1979 in Gdynia), and for waterbodies No. 2 and 3, it was 414 cm (registered on 04 November 1979 in Gdańsk-Port Północny). Zero ordinates for both gauging stations were referenced with sea level in Kronstadt (PL-KRON86-NH), thus with the very same height system, as in the case of depths registered by echosounders. Thanks to this data, it was possible to define depths corresponding to baselines at the surveyed waterbodies (d_{TSB}) [44]:

$$d_{TSB} = 5.08\ \text{m} - H_{LWL}, \quad (1)$$

where

H_{NSW}—the lowest water level in the PL-KRON86-NH system (m).

Over the final stage, the calculated isobaths (93 cm for waterbody No. 1 and 94 cm for waterbodies No. 2 and 3) were plotted onto seabed models in the form of TIN. Constant depth values were presented in the form of smooth curves, using a spline function.

2.5. TSB Variability Analysis

The next part was to evaluate the TSB variability in 2018–2020. The distance between baselines, as measured in particular years, was adopted as the measure of the change eval-

uation. For their determination, the Digital Shoreline Analysis System (DSAS) extension of ArcGiS software was used, allowing for the calculation of change statistics of boundaries between the land and water, based on time series [56,57]. The calculations started with the determination of the reference line in the form of [58]:

$$X_{RL} = b \cdot Y_{RL} + a, \tag{2}$$

where

X_{RL}, Y_{RL}—coordinates of the reference line in the PL-UTM system (m);
b—slope of the reference line (–);
a—x-intercept of the reference line (m).

The distance between the reference line and the TSB was then calculated. To do this, it was necessary to draw straight lines perpendicular to the reference line in the form of:

$$X_{PL_i} = -\frac{1}{b} \cdot Y_{PL_i} + a_i, \tag{3}$$

where

X_{PL_i}, Y_{PL_i}—coordinates of the i-th perpendicular line in the PL-UTM system (m);
i—numbering of perpendicular lines, increasing southwards (–);
a_i—mutual distance between successive perpendicular lines (m). For the purposes of this study, it was assumed to be 1 m.

The distances between the reference line and the baseline (d_i) were calculated based on the intersection points of these lines with the i-th perpendicular line:

$$d_i = \sqrt{\left(X_{RL_i} - X_{TSB_i}\right)^2 + \left(Y_{RL_i} - Y_{TSB_i}\right)^2}, \tag{4}$$

where

X_{RL_i}, Y_{RL_i}—reference line intersection points with the i-th perpendicular line in the PL-UTM system (m);
X_{TSB_i}, Y_{TSB_i}—TSB intersection points with the i-th perpendicular line in the PL-UTM system (m).

After calculating the distance between the reference line and the TSB from 2018–2020, the seasonal variability of the baseline in three representative waterbodies was determined. For this purpose, distances were calculated between two selected TSBs (Δd_i) using the following formula:

$$\Delta d_i = d_{2019-2020_i} - d_{2018-2019_i}, \tag{5}$$

where

$d_{2019-2020_i}$—distance between the TSB from 2019–2020 and the reference line calculated along the i-th perpendicular line (m),
$d_{2018-2019_i}$—distance between the TSB from 2018–2019 and the reference line calculated along the i-th perpendicular line (m).

Finally, the most frequently used statistical measure can be calculated, i.e., standard deviation of the distance between two selected TSBs from 2018–2020 ($\sigma_{\Delta d}$):

$$\Delta\overline{d} = \frac{\sum_{i=1}^{n} \Delta d_i}{n}, \tag{6}$$

$$\sigma_{\Delta d} = \sqrt{\frac{\sum_{i=1}^{n} \left(\Delta d_i - \Delta\overline{d}\right)^2}{n}}, \tag{7}$$

where

$\Delta\bar{d}$—arithmetic mean of the distances between two selected TSBs from 2018–2020 (m),
n—the number of perpendicular lines (–).

3. Results and Discussion

After measurement data elaboration, it was decided to visualize the TSB course, measured with USV in 2018–2020 in three representative waterbodies described in Table 1. The sea areas were an area adjacent to the public beach in Gdynia (Figure 5), an area located close to the Vistula Śmiała River mouth (Figure 6) and an area located at the approach to Górki Zachodnie from the Gdańsk Bay (Figure 7).

Figure 5. The course of the TSB of the waterbody adjacent to the public beach in Gdynia measured with the hydrographic method in 2018–2020.

Figure 6. The course of the TSB of the waterbody located close to the Vistula Śmiała River mouth measured with the hydrographic method in 2018–2020.

Figure 7. The course of the TSB of the waterbody located at the approach to Górki Zachodnie from the Gdańsk Bay measured with the hydrographic method in 2018–2020.

To determine the TSB variability at the three representative waterbodies in 2018–2020, it was decided to use the mathematical model presented in Section 2.5. With it, charts (Figures 8–10) were plotted, picturing how the baseline changed its location against the coastline over the course of years.

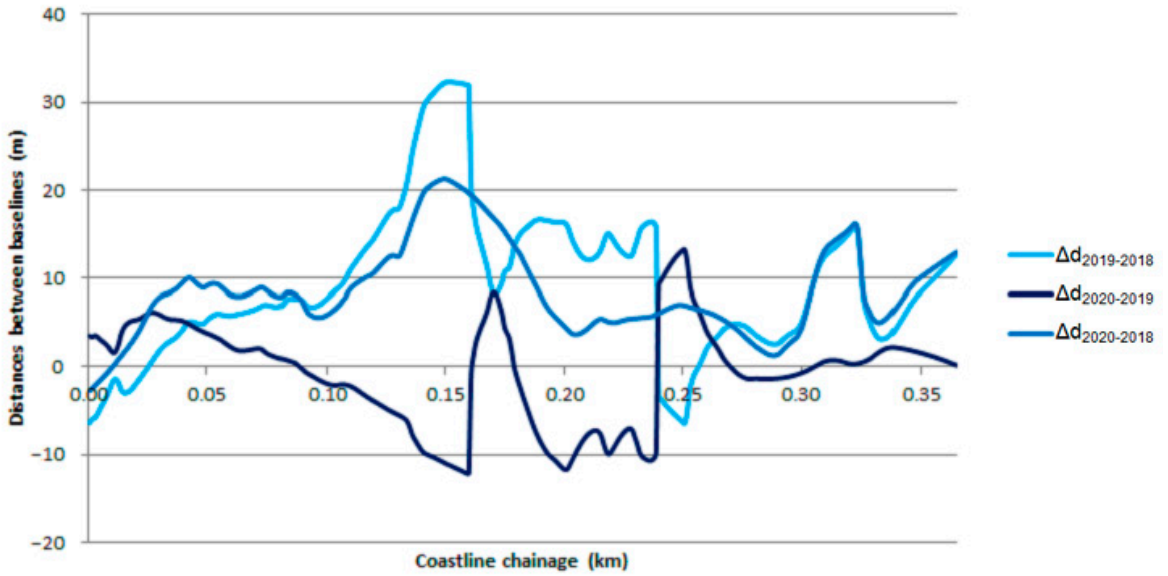

Figure 8. Distances between TSBs of the waterbody adjacent to the public beach in Gdynia measured with the hydrographic method in 2018–2020.

Figure 8 shows that the seasonal variability of the TSB course is quite considerable. The greatest differences were observed in the middle section of a waterbody, where the baseline moved up to 10 m for inland (coastline chainage: 0.145–0.16 and 0.19–0.24) in 2019–2020, and even moved towards the sea by up to 10–30 m (coastline chainage: 0.11–0.24) in 2018–2019. Moreover, it should be noted that the TSB changes irregularly (from −10 m to 10 m) along the coastline chainage. In order to determine, in a statistical context, how the baseline at the waterbody adjacent to the municipal beach in Gdynia had changed, it was decided to calculate the standard deviation in the distance between TSBs ($\sigma_{\Delta d}$).

This amounted to 8.37 m (in 2018–2019), 5.73 m (in 2019–2020) and 5.11 m (in 2018–2020). Undeniably, the main reason for the seasonal variability of the baseline course is the periodically performed land reclamation works in the area. As the authors of this paper managed to determine, the waterbody adjacent to the public beach in Gdynia is filled with material (sand) sourced during dredging of approach fairways to ports by the Maritime Authorities. The outcome of such actions are numerous "shallows" and "depressions" occurring up to an isobath of 1 m. An additional factor influencing the TSB variability is the waterbody seabed shape, which is characterized by the slowly rising depths when moving away from the coastline, and thus, at some points, the changes in the location of the baseline are considerable.

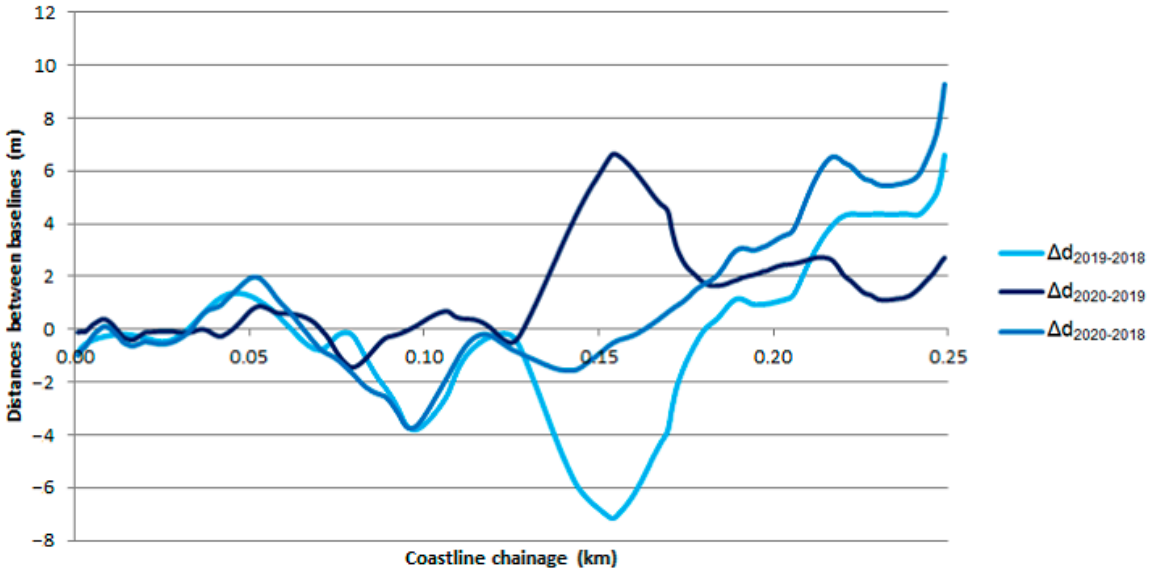

Figure 9. Distances between TSBs of the waterbody located close to the Vistula Śmiała River mouth measured with the hydrographic method in 2018–2020.

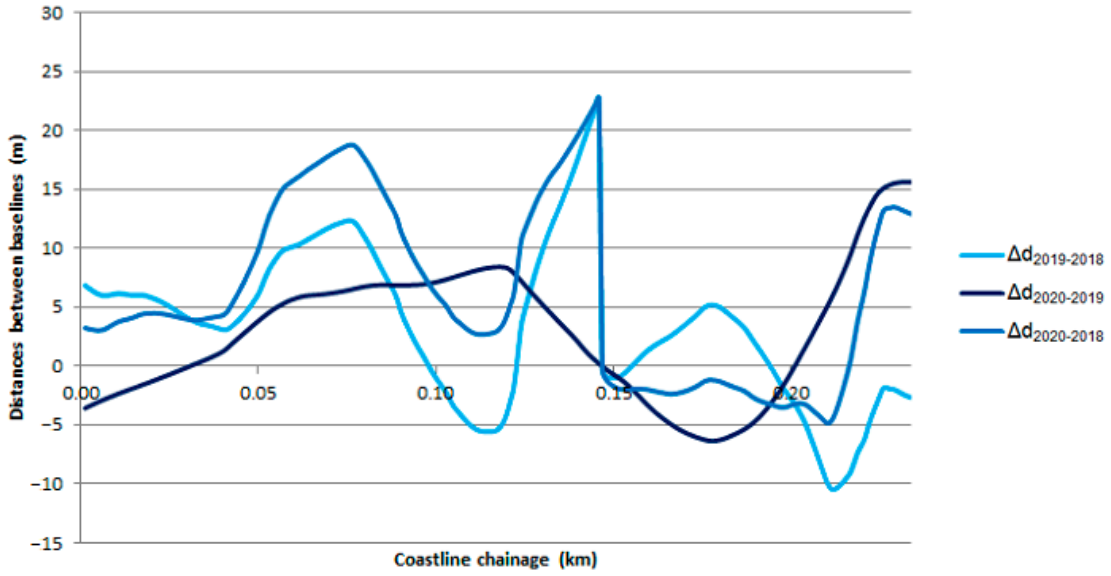

Figure 10. Distances between TSBs of the waterbody located at the approach to Górki Zachodnie from the Gdańsk Bay measured with the hydrographic method in 2018–2020.

Based on Figure 9, it may be noted that the seasonal variability of the TSB course is slight, as the baselines are almost overlapping one another. The greatest differences

were observed in the middle section of a waterbody, where the TSB moved up to approx. 5–7 m for inland (coastline chainage: 0.14–0.165) in 2018–2019, and even moved towards the sea by up to approx. 5–6 m (coastline chainage: 0.145–0.165) in 2019–2020. Excluding the middle section of the waterbody (coastline chainage: 0.14–0.17), it should be noted that the baseline changes irregularly (from −4 m to 4 m) along the coastline chainage. As in the case of the waterbody adjacent to the public beach in Gdynia, to determine, in a statistical context, how the TSB at the waterbody located near the Vistula Śmiała River mouth had changed, it was decided to calculate the standard deviation in the distance between baselines ($\sigma_{\Delta d}$). This amounted to 3.00 m (in 2018–2019), 1.86 m (in 2019–2020) and 2.80 m (in 2018–2020). The obtained statistical measures indicated that the location of the TSB is very stable. To a large degree, this stems from the fact that in some points (coastline chainage: 0.18–0.25), the waterbody features steep shores (within a couple of meters from the coastline, the depths amount up to 5 m), thus the changes on the baseline course are slight.

Figure 10 indicates that the seasonal variability of the TSB course is slight, with a few exceptions. The greatest differences were observed in the middle section of a waterbody, where the baseline moved up to a dozen or so meters towards the sea (coastline chainage: 0.13–0.145) in 2018–2019, and towards the sea by 10–15 m (coastline chainage: 0.22–0.235) in 2019–2020. Not counting the indicated locations, the TSB changed its location by a few meters, both inland, as well as towards the sea. As in the case of the previously presented waterbodies, to determine, in a statistical context, how the baseline at the waterbody located at the approach to Górki Zachodnie from the Gdańsk Bay had changed, it was decided to calculate the standard deviation in the distance between TSBs ($\sigma_{\Delta d}$). This amounted to 6.54 m (in 2018–2019), 5.54 m (in 2019–2020) and 7.57 m (in 2018–2020). Based on the obtained statistical measures, it must be stated that the location of the baseline is quite stable.

4. Conclusions

This paper aimed to define the TSB variability in 2018–2020. The survey was conducted in three representative waterbodies of the Republic of Poland: open sea, river mouth and exit from a large port, differing between each other in seabed shape.

Owing to the development of research tools, such as USVs, GNSS geodetic receivers and miniature echosounders, it is possible to take very accurate (1–5 cm, p = 0.95), detailed (the measurement coverage of the terrain being measured was much larger in comparison to classical geodetic methods) and rapid bathymetric measurements. This is of particular importance in ultra-shallow waters, since Poland's TSB is located at depths of tens of centimeters, up to 1–2 m below the current surface water level.

TSB measurements, carried out for three representative waterbodies of the Republic of Poland in 2018–2020, allowed to determine the seasonal variability of its course. Based on the obtained results, it was established that the smallest variability in the baseline course ($\sigma_{\Delta o_{2018-2019}} = 3.00$ m and $\sigma_{\Delta o_{2019-2020}} = 1.86$ m) was occurred in the waterbody near the Vistula Śmiała River mouth, which features steep shores (within a couple of meters from the coastline, there is a sudden increase of depth up to 5 m). For this reason, the changes in the location of the TSB are slight. On the other hand, the greatest variability in the baseline ($\sigma_{\Delta o_{2018-2019}} = 8.37$ m and $\sigma_{\Delta o_{2019-2020}} = 5.73$ m) was observed in the waterbody adjacent to the public beach in Gdynia. Factors conditioning considerable changes in TSB location included periodically performed land reclamation works at the area and the fact that the depth of the waterbody rises slowly when moving away from the coastline.

Author Contributions: Conceptualization, M.S. and C.S.; data curation, O.L. and M.W.; formal analysis, M.S. and Ł.M.; investigation, M.S. and Ł.M.; methodology, A.S. and M.P.-M.; supervision, C.S. and A.S.; visualization, O.L. and M.W.; writing—original draft, M.S. and C.S.; writing—review and editing, A.S. and M.P.-M. All authors have read and agreed to the published version of the manuscript.

Funding: This research was funded by the Ministry of Science and Higher Education in Poland, grant number DI2015 008545.

Conflicts of Interest: The authors declare no conflict of interest.

References

1. Klein, N. *Litigating International Law Disputes: Weighing the Options*; Cambridge University Press: New York, NY, USA, 2014.
2. Pina-Garcia, F.; Pereda-Garcia, R.; de Luis-Ruiz, J.M.; Perez-Alvarez, R.; Husillos-Rodriguez, R. Determination of Geometry and Measurement of Maritime-terrestrial Lines by Means of Fractals: Application to the Coast of Cantabria (Spain). *J. Coast. Res.* **2016**, *32*, 1174–1183. [CrossRef]
3. Abidin, H.Z.; Sutisna, S.; Padmasari, T.; Villanueva, K.J.; Kahar, J. Geodetic Datum of Indonesian Maritime Boundaries: Status and Problems. *Mar. Geod.* **2005**, *28*, 291–304. [CrossRef]
4. Horemuz, M. Error Calculation in Maritime Delimitation between States with Opposite or Adjacent Coasts. *Mar. Geod.* **1999**, *22*, 1–17. [CrossRef]
5. Ministry of Infrastructure and Development of the Republic of Poland. Justification of the Draft Ordinance of the Council of Ministers on the Detailed Course of the Baseline, External Boundary of the Territorial Sea and the External Boundary of Contiguous Zone of the Republic of Poland. Available online: https://www.senat.gov.pl/download/gfx/senat/pl/senatposiedzeniatematy/2737/drukisejmowe/3661.pdf (accessed on 17 April 2021). (In Polish)
6. UNCLOS. *United Nations Convention on the Law of the Sea of 10 December 1982*; UNCLOS: Montego Bay, Jamaica, 1982.
7. Council of Ministers of the Republic of Poland. *Ordinance of the Council of Ministers of 13 January 2017 on the Detailed Course of the Baseline, External Boundary of the Territorial Sea and the External Boundary of Contiguous Zone of the Republic of Poland*; Council of Ministers of the Republic of Poland: Warsaw, Poland, 2017. (In Polish)
8. Harsson, B.G.; Preiss, G. Norwegian Baselines, Maritime Boundaries and the UN Convention on the Law of the Sea. *Arct. Rev. Law Polit.* **2012**, *3*, 108–129.
9. Baptista, P.; Bastos, L.; Bernardes, C.; Cunha, T.; Dias, J. Monitoring Sandy Shores Morphologies by DGPS—A Practical Tool to Generate Digital Elevation Models. *J. Coast. Res.* **2008**, *24*, 1516–1528. [CrossRef]
10. Specht, C.; Weintrit, A.; Specht, M.; Dąbrowski, P. Determination of the Territorial Sea Baseline—Measurement Aspect. *IOP Conf. Ser. Earth Environ. Sci.* **2017**, *95*, 1–10. [CrossRef]
11. Kurowski, M.; Thal, J.; Damerius, R.; Korte, H.; Jeinsch, T. Automated Survey in Very Shallow Water Using an Unmanned Surface Vehicle. *IFAC PapersOnLine* **2019**, *52*, 146–151. [CrossRef]
12. Li, C.; Jiang, J.; Duan, F.; Liu, W.; Wang, X.; Bu, L.; Sun, Z.; Yang, G. Modeling and Experimental Testing of an Unmanned Surface Vehicle with Rudderless Double Thrusters. *Sensors* **2019**, *19*, 2051. [CrossRef]
13. Mu, D.; Wang, G.; Fan, Y.; Qiu, B.; Sun, X. Adaptive Trajectory Tracking Control for Underactuated Unmanned Surface Vehicle Subject to Unknown Dynamics and Time-varing Disturbances. *Appl. Sci.* **2018**, *8*, 547. [CrossRef]
14. Specht, M.; Specht, C.; Szafran, M.; Makar, A.; Dąbrowski, P.; Lasota, H.; Cywiński, P. The Use of USV to Develop Navigational and Bathymetric Charts of Yacht Ports on the Example of National Sailing Centre in Gdańsk. *Remote Sens.* **2020**, *12*, 2585. [CrossRef]
15. Stateczny, A.; Burdziakowski, P.; Najdecka, K.; Domagalska-Stateczna, B. Accuracy of Trajectory Tracking Based on Nonlinear Guidance Logic for Hydrographic Unmanned Surface Vessels. *Sensors* **2020**, *20*, 832. [CrossRef]
16. Stateczny, A.; Kazimierski, W.; Burdziakowski, P.; Motyl, W.; Wisniewska, M. Shore Construction Detection by Automotive Radar for the Needs of Autonomous Surface Vehicle Navigation. *Int. J. Geo Inf.* **2019**, *8*, 80. [CrossRef]
17. Wróbel, K.; Weintrit, A. With Regard to the Autonomy in Maritime Operations—Hydrography and Shipping, Interlinked. *TransNav Int. J. Mar. Navig. Saf. Sea Transp.* **2020**, *14*, 745–749. [CrossRef]
18. Yang, Y.; Li, Q.; Zhang, J.; Xie, Y. Iterative Learning-based Path and Speed Profile Optimization for an Unmanned Surface Vehicle. *Sensors* **2020**, *20*, 439. [CrossRef] [PubMed]
19. Bažec, M.; Dimc, F.; Pavlovčič-Prešeren, P. Evaluating the Vulnerability of Several Geodetic GNSS Receivers under Chirp Signal L1/E1 Jamming. *Sensors* **2020**, *20*, 814. [CrossRef] [PubMed]
20. Krasuski, K.; Savchuk, S. Determination of the Precise Coordinates of the GPS Reference Station in of a GBAS System in the Air Transport. *Commun. Sci. Lett. Univ. Zilina* **2020**, *22*, 11–18. [CrossRef]
21. Paziewski, J.; Sieradzki, R.; Baryla, R. Multi-GNSS High-rate RTK, PPP and Novel Direct Phase Observation Processing Method: Application to Precise Dynamic Displacement Detection. *Meas. Sci. Technol.* **2018**, *29*, 91001. [CrossRef]
22. Šakan, D.; Kos, S.; Ban, B.D.; Brčić, D. On Linear and Circular Approach to GPS Data Processing: Analyses of the Horizontal Positioning Deviations Based on the Adriatic Region IGS Observables. *Data* **2021**, *6*, 9. [CrossRef]
23. Žic, A.; Pongračić, B.; Kos, S.; Brčić, D. On GPS L1 Positioning Errors' Estimation in the Adriatic Region. *Pomorski Zbornik* **2020**, *58*, 169–184.
24. Jin, J.; Zhang, J.; Shao, F.; Lv, Z.; Li, M.; Liu, L.; Zhang, P. Active and Passive Underwater Acoustic Applications Using an Unmanned Surface Vehicle. In Proceedings of the OCEANS 2016—Shanghai, Shanghai, China, 10–13 April 2016.
25. Seto, M.L.; Crawford, A. Autonomous Shallow Water Bathymetric Measurements for Environmental Assessment and Safe Navigation Using USVs. In Proceedings of the OCEANS 2015—MTS/IEEE Washington, Washington, DC, USA, 19–22 October 2015.

26. Stateczny, A.; Burdziakowski, P. Universal Autonomous Control and Management System for Multipurpose Unmanned Surface Vessel. *Pol. Marit. Res.* **2019**, *26*, 30–39. [CrossRef]
27. Wlodarczyk-Sielicka, M.; Stateczny, A. Comparison of Selected Reduction Methods of Bathymetric Data Obtained by Multibeam Echosounder. In Proceedings of the 2016 Baltic Geodetic Congress, Gdańsk, Poland, 2–4 June 2016.
28. Zwolak, K.; Wigley, R.; Bohan, A.; Zarayskaya, Y.; Bazhenova, E.; Dorshow, W.; Sumiyoshi, M.; Sattiabaruth, S.; Roperez, J.; Proctor, A.; et al. The Autonomous Underwater Vehicle Integrated with the Unmanned Surface Vessel Mapping the Southern Ionian Sea. The Winning Technology Solution of the Shell Ocean Discovery XPRIZE. *Remote Sens.* **2020**, *12*, 1344. [CrossRef]
29. El-Hattab, A.I. Investigating the Effects of Hydrographic Survey Uncertainty on Dredge Quantity Estimation. *Mar. Geod.* **2014**, *37*, 389–403. [CrossRef]
30. Jang, W.S.; Park, H.S.; Seo, K.Y.; Kim, Y.K. Analysis of Positioning Accuracy Using Multi Differential GNSS in Coast and Port Area of South Korea. *J. Coast. Res.* **2016**, *75*, 1337–1341. [CrossRef]
31. Specht, C.; Specht, M.; Cywiński, P.; Skóra, M.; Marchel, Ł.; Szychowski, P. A New Method for Determining the Territorial Sea Baseline Using an Unmanned, Hydrographic Surface Vessel. *J. Coast. Res.* **2019**, *35*, 925–936. [CrossRef]
32. Angnuureng, D.B.; Jayson-Quashigah, P.-N.; Almar, R.; Stieglitz, T.C.; Anthony, E.J.; Aheto, D.W.; Addo, K.A. Application of Shore-based Video and Unmanned Aerial Vehicles (Drones): Complementary Tools for Beach Studies. *Remote Sens.* **2020**, *12*, 394. [CrossRef]
33. Casella, E.; Drechsel, J.; Winter, C.; Benninghoff, M.; Rovere, A. Accuracy of Sand Beach Topography Surveying by Drones and Photogrammetry. *Geo Mar. Lett.* **2020**, *40*, 255–268. [CrossRef]
34. Contreras-de-Villar, F.; García, F.J.; Muñoz-Perez, J.J.; Contreras-de-Villar, A.; Ruiz-Ortiz, V.; Lopez, P.; Garcia-López, S.; Jigena, B. Beach Leveling Using a Remotely Piloted Aircraft System (RPAS): Problems and Solutions. *J. Mar. Sci. Eng.* **2021**, *9*, 19. [CrossRef]
35. Genchi, S.A.; Vitale, A.J.; Perillo, G.M.E.; Seitz, C.; Delrieux, C.A. Mapping Topobathymetry in a Shallow Tidal Environment Using Low-cost Technology. *Remote Sens.* **2020**, *12*, 1394. [CrossRef]
36. Lowe, M.K.; Adnan, F.A.F.; Hamylton, S.M.; Carvalho, R.C.; Woodroffe, C.D. Assessing Reef-island Shoreline Change Using UAV-derived Orthomosaics and Digital Surface Models. *Drones* **2019**, *3*, 44. [CrossRef]
37. Kim, H.; Lee, S.B.; Min, K.S. Shoreline Change Analysis Using Airborne LiDAR Bathymetry for Coastal Monitoring. *J. Coast. Res.* **2017**, *79*, 269–273. [CrossRef]
38. Alcaras, E.; Parente, C.; Vallario, A. Automation of Pan-Sharpening Methods for Pléiades Images Using GIS Basic Functions. *Remote Sens.* **2021**, *13*, 1550. [CrossRef]
39. Al-Mansoori, S.; Al-Marzouqi, F. Coastline Extraction Using Satellite Imagery and Image Processing. *Techniques. Int. J. Curr. Eng. Technol.* **2016**, *6*, 1245–1251.
40. Maglione, P.; Parente, C.; Vallario, A. Coastline Extraction Using High Resolution WorldView-2 Satellite Imagery. *Eur. J. Remote Sens.* **2014**, *47*, 685–699. [CrossRef]
41. Wang, X.; Liu, Y.; Ling, F.; Liu, Y.; Fang, F. Spatio-temporal Change Detection of Ningbo Coastline Using Landsat Time-series Images during 1976–2015. *ISPRS Int. J. Geo Inf.* **2017**, *6*, 68. [CrossRef]
42. Viaña-Borja, S.P.; Ortega-Sánchez, M. Automatic Methodology to Detect the Coastline from Landsat Images with a New Water Index Assessed on Three Different Spanish Mediterranean Deltas. *Remote Sens.* **2019**, *11*, 2186. [CrossRef]
43. Xu, N. Detecting Coastline Change with All Available Landsat Data over 1986–2015: A Case Study for the State of Texas, USA. *Atmosphere* **2018**, *9*, 107. [CrossRef]
44. Specht, M.; Specht, C.; Wąż, M.; Naus, K.; Grządziel, A.; Iwen, D. Methodology for Performing Territorial Sea Baseline Measurements in Selected Waterbodies of Poland. *Appl. Sci.* **2019**, *9*, 3053. [CrossRef]
45. IHO. *IHO Standards for Hydrographic Surveys*, 6th ed.; IHO Publication No. 44; IHO: Monte Carlo, Monaco, 2020.
46. Marchel, Ł.; Specht, C.; Specht, M. Assessment of the Steering Precision of a Hydrographic USV along Sounding Profiles Using a High-precision GNSS RTK Receiver Supported Autopilot. *Energies* **2020**, *13*, 5637. [CrossRef]
47. Specht, M.; Specht, C.; Lasota, H.; Cywiński, P. Assessment of the Steering Precision of a Hydrographic Unmanned Surface Vessel (USV) along Sounding Profiles Using a Low-cost Multi-Global Navigation Satellite System (GNSS) Receiver Supported Autopilot. *Sensors* **2019**, *19*, 3939. [CrossRef]
48. Grządziel, A. Single Beam Echo Sounder in Hydrographic Surveys. *Marit. Rev.* **2006**, *4*, 11–28. (In Polish)
49. Cignoni, P.; Montani, C.; Perego, R.; Scopigno, R. Parallel 3D Delaunay Triangulation. *Comput. Graph. Forum* **1993**, *12*, 129–142. [CrossRef]
50. Cohen-Steiner, D.; de Verdiere, E.C.; Yvinec, M. Conforming Delaunay Triangulations in 3D. *Comput. Geom.* **2004**, *28*, 217–233. [CrossRef]
51. Fang, T.-P.; Piegl, L.A. Delaunay Triangulation in Three Dimensions. *IEEE Comput. Graph. Appl.* **1995**, *15*, 62–69. [CrossRef]
52. Liu, Y.; Lo, S.H.; Guan, Z.-Q.; Zhang, H.-W. Boundary Recovery for 3D Delaunay Triangulation. *Finite Elem. Anal. Des.* **2014**, *84*, 32–43. [CrossRef]
53. Lihua, Z.; Shuaidong, J.; Rencan, P.; Jian, D.; Ning, L. A Quantitative Method to Control and Adjust the Accuracy of Adaptive Grid Depth Modeling. *Mar. Geod.* **2013**, *36*, 408–427. [CrossRef]
54. Makar, A. The Sea Bottom Surface Described by Coons Pieces. *Sci. J. Marit. Univ. Szczec.* **2016**, *45*, 187–190.
55. Sassais, R.; Makar, A. Methods to Generate Numerical Models of Terrain for Spatial ENC Presentation. *Annu. Navig.* **2011**, *18*, 69–81.

56. Mujabar, S.; Chandrasekar, N. A Shoreline Change Analysis along the Coast between Kanyakumari and Tuticorin, India, Using Digital Shoreline Analysis System. *Geo Spat. Inf. Sci.* **2011**, *14*, 282–293.
57. Specht, M.; Specht, C.; Lewicka, O.; Makar, A.; Burdziakowski, P.; Dąbrowski, P. Study on the Coastline Evolution in Sopot (2008–2018) Based on Landsat Satellite Imagery. *J. Mar. Sci. Eng.* **2020**, *8*, 464. [CrossRef]
58. Specht, M.; Specht, C.; Wąż, M.; Dąbrowski, P.; Skóra, M.; Marchel, Ł. Determining the Variability of the Territorial Sea Baseline on the Example of Waterbody Adjacent to the Municipal Beach in Gdynia. *Appl. Sci.* **2019**, *9*, 3867. [CrossRef]